CLAWAR 2019: 22nd International Conference on
Climbing and Walking Robots and the Support
Technologies for Mobile Machines,
Kuala Lumpur, Malaysia, 26-28 August 2019.
https://doi.org/10.13180/clawar.2019.26-28.08.09

MINIATURIZATION OF ULTRASONIC MOTOR AND ROTOR BLADE FOR ROTARY-WING MICRO AERIAL VEHICLE

ERIC TAN KAI CHIANG and TOMOAKI MASHIMO
Mechanical Engineering Department, Toyohashi University of Technology, Tempaku-cho
Toyohashi, Aichi, 441-8580, Japan
E-mail: erictan@is.me.tut.ac.jp, mashimo@me.tut.ac.jp
http://eiiris.tut.ac.jp/mashimo/wordpress/

Micro actuator and micro rotor blade are important elements when developing a rotary-wing micro aerial vehicle (MAV). We propose a micro ultrasonic motor with a 1mm cube stator and design a micro rotor blade with 5mm wingspan. The trial production of both the micro ultrasonic motor and micro rotor blade is carried out. The prototype micro rotor blade is attached to the prototype micro ultrasonic motor and drive experiment is conducted to test the performance of the assembled device. A micro soldering equipment is also developed to produce stable solder results for the assembled device. Experimental result shows the transient response of rotational speed of the device.

1. Introduction

Japan is a country with a lot of natural disasters such as earthquakes, typhoons, and tsunamis. During the occurrence of natural disaster, it is necessary to confirm the existence of survivors and to collect information in places where people could not reach. Developing a small flying robot is one of the most optimum way to carry out this mission. At present, studies on flying robots, or commonly known as unmanned aerial vehicles (UAV [1]) for collecting such information have been carried out by many research institutes, universities and colleges. Among those, study on micro aerial vehicles (MAV [2]), which are extremely small in size that can fly freely even in narrow spaces, is getting more and more attention in this modern society. MAV is defined as a flying robot with a wingspan of approximately 15cm or less. The key to developing a highly practical MAV is miniaturization. Currently, the smallest MAVs in the world include flapping type MAV, RoboBee [3] (wingspan: 3.0cm) and rotating type MAV, Piccolissimo [4] (wingspan: 2.8cm). To miniaturize MAV to even smaller, what is particularly problematic is that the performance of the actuator and rotor blade is insufficient for the flying robot to take off. Thus, in this paper, we described the trial production of the micro ultrasonic motor and micro rotor blade developed in this laboratory, aiming to develop the smallest MAV in the world.

2. Micro Ultrasonic Motor

The ultrasonic motor is advantageous for miniaturization because it has a larger torque that can be generated per volume, and has a simple structure and excellent machinability compared to other motor drive principles. The miniaturization of ultrasonic motors has been carried out in the past by universities and research institutes [5], [6]. However, in many cases, when it was miniaturized to a size of about 1 mm, only a torque that could barely rotate could be obtained. In other words, when a rotor blade is attached, the load torque will increase and the motor might not be able to rotate. The micro ultrasonic motor developed in this laboratory can be

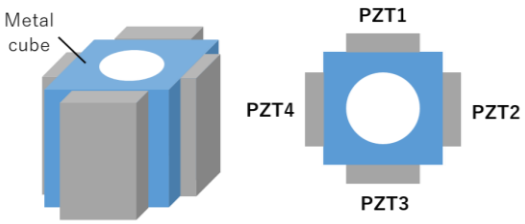

Figure 1. Schematic of micro ultrasonic motor

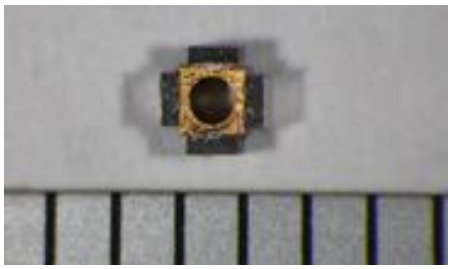

Figure 2. Prototype micro ultrasonic motor

manufactured on a trial basis with a size of about 1mm, and is a motor that can generate a torque (about 10μNm) of a practical level to a certain extent [7], [8].

2.1. *Driving Principle*

The micro ultrasonic motor developed in this laboratory is a motor driven using the piezoelectric effect. As shown in fig. 1, four piezoelectric elements (PZT1 to PZT4) are attached to the four faces of a metal cube with a through hole. Generally, since the vibration amplitude of the piezoelectric element is very small, in the case of micro ultrasonic waves, the amplitude is amplified using the vibration mode of three waves on the inner circumferential surface. The merit of using such a vibration mode is that the axial dimension of the stator does not depend on the natural frequency. That is, even if the actuator is not shaped as in the conventional actuator, the natural frequency is constant, and a certain magnitude of vibration amplitude and torque can be generated. This means that the shape design of the stator has the advantage of having a certain degree of freedom.

2.2. *Design and Trial Production*

The prototype stator is shown in fig. 2. To develop a motor about 1mm in size, it is important to have a design that can be prototyped. In other words, it is important to be able to process the metal and the piezoelectric material that make up the stator, and to be able to assemble those parts. Phosphor bronze, which has excellent formability, is used as the metal part of the stator. The metal part of the stator is a 1.0mm square cube with a hole of 0.7mm in diameter for passing the rotor. Four piezoelectric elements are attached to the four side surfaces of the stator, and the size of the piezoelectric element is 1.0mm × 0.8mm × 0.3mm. An electrically conductive epoxy adhesive is used to bond the metal cube and piezoelectric elements. Through this method, it is possible to trial produce a stator with a simple structure without relying on processing technology or special materials.

2.3. *Impedance Analysis*

To evaluate the performance of the prototype stator, it is necessary to investigate the frequency characteristics of impedance of the stator using an impedance analyzer. The electric wires of the impedance analyzer were connected to the piezoelectric elements PZT1 and PZT3 and the change in impedance from a frequency of 900 kHz to 1100 kHz was investigated. Similar measurements were performed on the piezoelectric elements PZT2 and PZT4. From the results in fig. 3, the error of the resonant frequency of less than 1% is obtained. Thus, it is considered that the prototype micro ultrasonic motor can rotate well as described in the driving principle.

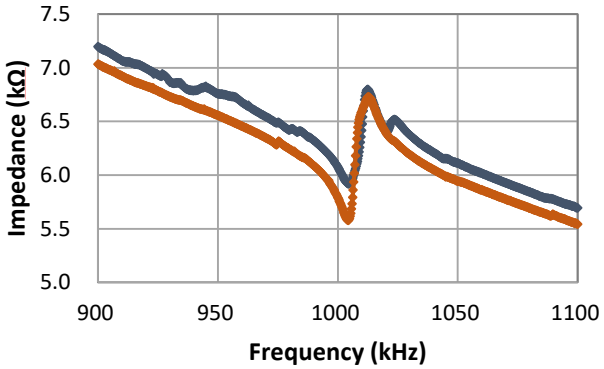

Figure 3. Frequency characteristics of impedance

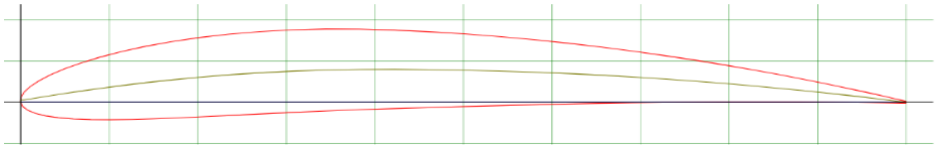

Figure 4. NACA 4410

3. Micro Rotor Blade

To develop the target MAV, a rotor blade with a wingspan of 10mm or less is required. However, it is impossible to purchase such a small rotor blade from current market. Hence, in this paper, we design a micro rotor blade and carry out the trial production using a 3D printer with an accuracy of 16μm.

3.1. *Selection of Airfoil and Airfoil Analysis*

Airfoil refers to the cross-sectional shape of a wing, blade (propeller, rotor, turbine) or ship sail. To design a propeller, it is necessary to determine the airfoil. There are various types of airfoil shapes, but for this design, we selected the shape of the most commonly used airfoil named NACA4-Digit. The characteristics of this airfoil are its simplicity and few parameters. The shape of NACA 4-Digit consists of four digits, and each number indicates the size of the camber, the position of the camber, and the wing thickness ratio respectively [9]. NACA 4410 shown in fig. 4 was selected as the cross-sectional shape for designing the micro rotor blade. Beside airfoil shape, attack angle is important too when comes to designing rotor blade. By properly determining the attack angle of each part of the wing, the lift-drag ratio of the micro rotor blade can be maximized, and better flight performance can be achieved. In this study, the analysis of the selected NACA 4410 airfoil is performed using analysis software called xflr5 developed at MIT, and the attack angle of each part is determined. xflr5 is an analysis tool for airfoils, wings and planes operating at low Reynolds numbers. To carry out the analysis, it is necessary to calculate the Reynolds number of each part of the rotor blade. When Reynolds number is expressed as Re, the following equation is obtained.

$$\mathrm{Re} = \frac{Vc}{1000\nu} \tag{1}$$

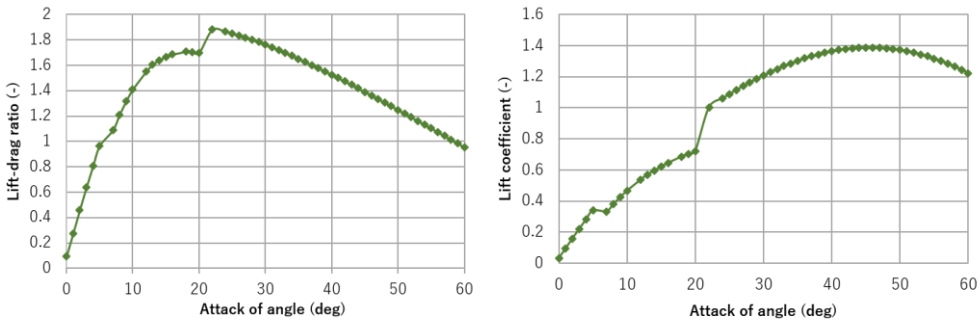

(a) Lift-drag ratio (b) Lift coefficient

Figure 5. Analysis results of xflr5

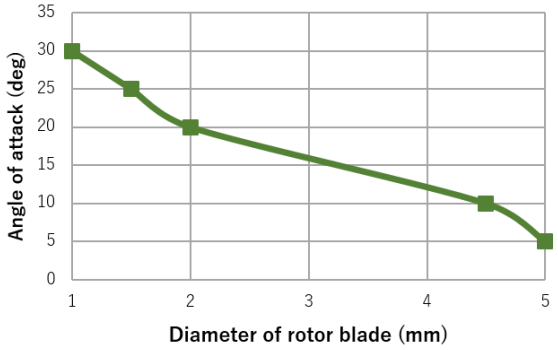

Figure 6. Selection of attack angles for rotor blade

Here, V is the rotational speed of the rotor blade, c is the chord of the airfoil, v is the kinematic viscosity, and V is expressed as the following equation.

$$\mathrm{V} = \frac{\pi n}{60} \times \frac{\pi D}{1000} \tag{2}$$

Here, n is the rotational speed of the actuator, and D is the wingspan of the rotor blade. First, the calculated Reynolds number is input to the analysis software, and the analysis results shown in Fig. 5 are obtained. From Fig. 5(a), the angle of attack when the lift-drag ratio is at maximum obtained, and the lift coefficient of that attack angle is obtained from fig. 5(b). The lift coefficient is then being used to calculate the lift force, F_L, by using the following equation.

$$F_L = \frac{1}{2}\rho v^2 A C_L \tag{3}$$

Here, ρ is the air density, v is the speed of rotor blade, A is the surface area of rotor blade, and C_L is the lift coefficient obtained from the graphs. Figure 6 shows the selection of the attack angle based on the analysis results of xflr5. Attack angles where lift-drag ratio is at the highest are selected for most parts except at the tip of rotor blade. This is because the higher the angle of attack at the tip of the rotor blade, the more easily the tip vortex occurs. Tip vortices are phenomena in which the flow of air from the side of the wing occurs to fill the pressure difference between the upper and lower surfaces, and the lift force drops sharply. Therefore, the attack angles at the tip of the rotor blade are being set as low as possible to prevent the occurrence of tip vortex.

Figure 7. Prototype micro rotor blade

Figure 8. Micro soldering equipment

3.2. *Design and Trial Production*

In this study, the wingspan is set to 5.0mm and the number of blades is set to two to lighten the flight device. The designed rotor blade was prototyped using a 3D printer with a laminated pitch of 16μm. The prototype micro rotor blade is shown in fig 7. The lift force of the prototype micro rotor blade is estimated to be 0.48mN using Eq. (3). Since the total mass of the device is 0.36mN, it is theoretically considered that the lift force of the designed rotor blade is sufficient for the flight of the device.

4. Drive Experiment of the Device

4.1. *Assembly of the Device*

In addition to the stator, a rotor, a spring, a preload mechanism and a stopper are used for assembling the micro ultrasonic motor. The assembled micro ultrasonic motor and the prototype micro rotor blade are then assembled by using ThreeBond 1537 adhesive as the bonding paste. The characteristic of the adhesive is that it can be easily removed from the parts, so that it can be easily replaced with another rotor blade of different design in the future. To conduct drive experiments of the assembled device, it is necessary to solder the wires to the four piezoelectric elements attached to the device. It is desirable to create an environment that enables soldering as stable as possible to reduce the influence of soldering on the performance of the prototype

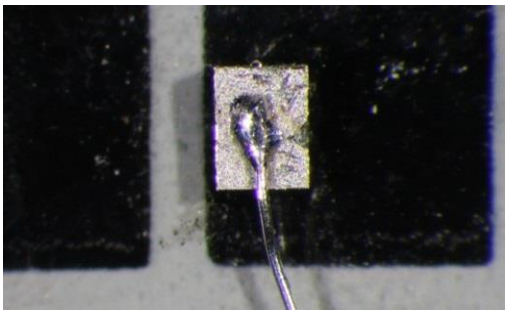

Figure 9. Stable soldering result

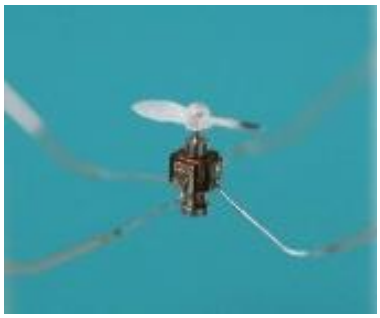

Figure 10. Assembled and soldered device

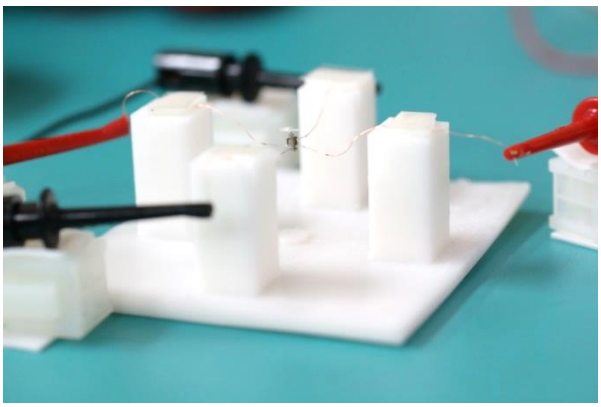

Figure 11. Experimental setup for drive experiment

micro ultrasonic motor. However, it is difficult to stably solder a 0.3mm electric wire to a 1.0mm × 0.8mm × 0.3mm piezoelectric element. Thus, in this study, we developed a micro soldering equipment shown in fig 8, to solve the problem. With this equipment, it is possible to finely adjust the position of soldering to the piezoelectric element and the amount of solder. Fig. 9 shows the stable soldering results obtained using the equipment. The device assembled and soldered is shown in fig. 10.

4.2. *Drive Experiment*

The experimental setup shown in fig. 11 was prepared to conduct the drive experiment of the device. A voltage of 120Vpp and frequency of 974kHz were applied to drive the device. This frequency is the value previously adjusted so that the motor rotates at the best. The method of measuring the number of revolutions using a rotary encoder is most commonly used in robotics field. However, in the case of a micromotor, the moment of inertia and the viscous friction of the rotary encoder are relatively large, which affects the performance of the motor. Therefore, we adopt a method to capture the rotation of the device's rotor blade using a high-speed camera without touching it. Markers are attached to the surface of the rotor blade, and the motion of the rotor blade is tracked by image processing. The rotational speed is then calculated from the angular displacement obtained for each image. Fig. 12 shows the transient response of the rotational speed of the device captured with a high-speed camera (frame rate: 6000 fps) when a voltage of 120Vpp is applied. A stable rotational speed of about 6000rpm was obtained in about 0.12 seconds from the start of the device rotation. From the drive experiment, we confirmed the

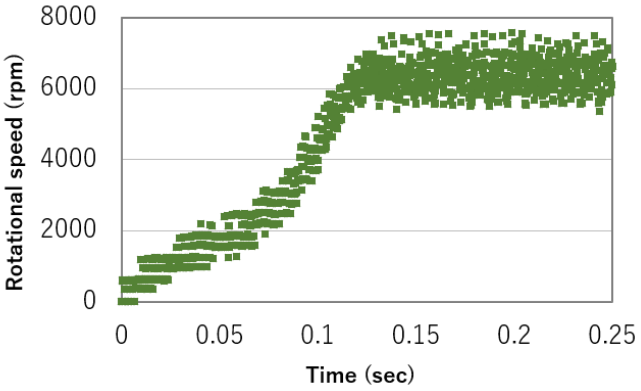

Figure 12. Transient response of rotational speed

rotation of the device, but we could not confirm the flight. The reason is that the lift force generated by the rotor blade is insufficient for the flight of the device, which means that the actual lift force generated is different from the theoretically calculated lift force. Thus, as future plan, we will measure the actual lift force generated by the rotor blade and compare it with the theoretical value. From there, considering the percentage drop from the theoretical lift force value, we will change the design of the rotor blade to generate enough lift force to support the weight of the device, and conduct the same experiment again to evaluate the flight performance.

Acknowledgments

This work is supported by JSPS KAKENHI 16H06075.

References

1. F. Bohorquez, P. Samuel, J. Sirohi, D. Pines and L. Rudd, “Design, Analysis and Hover Performance of a Rotary Wing Micro Air Vehicle,” Journal of the American Helicopter Society, vol. 48-no. 2, pp.80-90, 2003
2. S.M. Ettinger, M. C. Nechyba, P. G. Ifju and M. Waszak, “Vision-Guided Flight Stability and Control for Micro Air Vehicles,” IEEE/RSJ International Conference on Robots and Systems, pp.2134-2140, 2002
3. R.J. Wood, “Liftoff of 60mg flapping-wing MAV,” IEEE/RSJ International Conference on intelligent Robots and Systems, pp.1889-1894, 2007
4. Matthew Piccoli and Mark Yim, “Piccolissimo: The smallest micro aerial vehicle,” IEEE International Conference on Robotics and Automation (ICRA),” pp.3328-3333, 2017
5. T. Morita, “Miniature piezoelectric motors,” Sensors and Actuators A: Physical, vol. 103, pp.291-300, 2003
6. K. Uchino, S. Cagatay, B. Koc, S. Dong, P. Bouchilloux and M. Strauss, “Micro Piezoelectric Ultrasonic Motors,” Journal of Electroceramics, vol. 13, pp.393-401, 2004
7. T. Mashimo, “Performance of micro ultrasonic motor using one cubic millimeter stator,” IEEE International Ultrasonics Symposium, IUS, vol.213, pp.866-869, 2014
8. T. Mashimo, “Miniature preload mechanisms for a micro ultrasonic motor,” Sensors and Actuators A: Physical, vol.257, pp.106-112, 2017
9. E. N. Jacobs, K. E. Ward and R. M. Pinkerton, “The characteristics of 78 related airfoil sections from tests in the variable-density wind tunnel,” NACA, 1933